Buletin Ilmiah Sarjana Teknik Elektro
Vol. 8, No. 5, October 2026, pp. 1659-1674
ISSN: 2685-9572, DOI: 10.12928/biste.v8i5.15850

BAT-Optimized Adaptive Backstepping Control for a Two-Degree-of-Freedom Prosthetic Knee: Dynamic Modeling and Simulation Study

Mayyasah Ali Salman [1], **Israa Saad Khalid** [2], **Rawaa Abdal-Sattar Ali** [2], **Hadeel Ghalib Abbas** [3], **Zubaida Muhammad Saad Al Din Khalil** [2], Saleem Khalefa Kadhim [4], **Aws M. Abdullah** [2]
[1] Department of Electronic and Communications Engineering, College of Engineering, Al-Nahrain University, Baghdad 10071, Iraq
[2] Department of Banking and Financial Sciences, College of Islamic Sciences, University of Baghdad, Iraq
[3] History Department, Ibn Rushed College of Education for Humanitarian Studies, University of Baghdad, Iraq
[4] Department of Intelligent Robotics Engineering, College of Artificial Intelligent Engineering, University of Technology-Iraq, Baghdad 10066, Iraq

ARTICLE INFORMATION

Article History:

Received 15 January 2026
Revised 26 March 2026
Accepted 04 November 2026

Keywords:

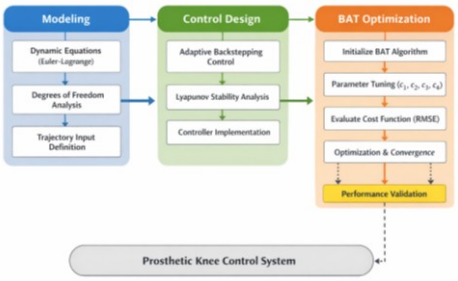
Prosthetic Knee Control;
Backstepping Controller;
ABS Controller;
BAT Algorithm;
Lower Limb Amputation
Prosthetic Knee Joint

Corresponding Author:

Saleem Khalefa Kadhim,
Department of Intelligent Robotics Engineering, College of Artificial Intelligent Engineering, University of Technology-Iraq, Baghdad 10066, Iraq.
Email:
Saleem.K.Kadhim@uotechnology.edu.iq

This work is open access under a Creative Commons Attribution-Share Alike 4.0

ABSTRACT



This study addresses mobility limitations experienced by individuals with transfemoral lower-limb amputations, particularly during turning and uneven terrain navigation. A two-degree-of-freedom prosthetic knee mechanism is proposed to enhance internal, external rotation control of the thigh, shank system during both stance and swing phases of gait. The main contribution of this research is the integration of BAT-optimized Adaptive Backstepping control to improve trajectory tracking and robustness under nonlinear dynamics and disturbances. A nonlinear dynamic model of the prosthetic knee is derived using the Euler–Lagrange formulation, which is selected for its suitability in multi-link biomechanical systems. Both Backstepping and Adaptive Backstepping controllers are designed based on Lyapunov stability theory, while the BAT algorithm is employed to automatically tune controller parameters and avoid trial-and-error tuning. Simulation scenarios include sinusoidal reference trajectories with external disturbances and uncertain parameters. The proposed BAT-optimized Adaptive Backstepping controller demonstrates improved performance compared with the optimized Backstepping controller. Quantitative results show a reduction in position tracking error with improvement rates of 11.1% for the thigh and 3.4% for the shank. These findings indicate enhanced robustness and tracking accuracy. The study is limited to simulation-based validation, and future work will focus on experimental implementation and real-time control of prosthetic knee systems.

Document Citation:

M. A. Salman, I. S. Khalid, R. A.-S. Ali, H. G. Abbas, Z. M. S. A. D. Khalil, S. K. Kadhim, and A. M. Abdullah, "BAT-Optimized Adaptive Backstepping Control for a Two-Degree-of-Freedom Prosthetic Knee: Dynamic Modeling and Simulation Study," *Buletin Ilmiah Sarjana Teknik Elektro*, vol. 8, no. 5, pp. 1659-1674, 2026, DOI: 10.12928/biste.v8i5.15850.

1. INTRODUCTION

Lower-limb amputation has a profound impact on mobility, balance, and overall quality of life, particularly for individuals with transfemoral amputations who depend on prosthetic knee joints for routine activities. Achieving smooth and reliable motion throughout both stance and swing phases remains a major challenge in prosthetic knee design, especially during turning maneuvers or movement on uneven surfaces. Many conventional prosthetic knees are limited in degrees of freedom, which restricts natural limb motion and reduces user comfort. The absence of adequate internal–external rotational capability often forces users to adopt compensatory strategies, increasing energy expenditure and potentially causing long-term musculoskeletal issues [1]–[3]. Consequently, developing advanced control strategies for multi-degree-of-freedom prosthetic knees has become an important research direction.

Numerous control techniques have been investigated to enhance prosthetic knee performance. Classical linear controllers, such as proportional–integral–derivative (PID), are commonly used because of their simplicity; however, they are not well suited for highly nonlinear biomechanical systems and uncertain operating conditions [4][5]. To improve performance, researchers have explored nonlinear approaches including Sliding Mode Control (SMC), feedback linearization, and adaptive control strategies [6]–[8]. While SMC provides robustness to disturbances, it may introduce chattering that is undesirable in biomechanical applications [9]. Feedback linearization depends heavily on accurate system models and can degrade when uncertainties are present [10]. Adaptive control techniques address some of these limitations by adjusting parameters online, thereby improving robustness against system variations [11][12].

Among nonlinear techniques, Backstepping control has gained attention due to its Lyapunov-based recursive design procedure and suitability for strict-feedback nonlinear systems [13][14]. Adaptive Backstepping further enhances this framework by incorporating parameter adaptation to handle uncertainties and external disturbances [15]. Although these approaches have been applied to robotic and prosthetic systems, many implementations rely on manually selected controller parameters, which may not achieve optimal performance and often require extensive trial-and-error tuning [16][17]. This limitation motivates the use of automated optimization methods.

Metaheuristic optimization algorithms have therefore been introduced for controller tuning. Techniques such as Particle Swarm Optimization (PSO), Genetic Algorithm (GA), and Grey Wolf Optimizer (GWO) have shown promising results in biomechanical and robotic applications [18]–[20]. However, these algorithms may suffer from slow convergence or local optima depending on the problem characteristics. The Bat Algorithm (BAT), inspired by the echolocation behavior of bats, offers strong global search capability and efficient convergence properties [21]. Despite its potential advantages, the application of BAT for tuning Adaptive Backstepping controllers in multi-degree-of-freedom prosthetic knee systems remains limited [22].

Additionally, many existing studies focus on single-degree-of-freedom prosthetic knee models and neglect internal–external rotational dynamics. Several works also rely solely on simulation-based validation or provide limited evaluation under disturbances and uncertainties, which reduces confidence in real-world applicability [23]. Reported limitations include insufficient consideration of multi-degree-of-freedom dynamics, computational challenges in real-time implementations, lack of comprehensive comparisons among advanced controllers, reduced robustness under unstructured uncertainties, and limited experimental validation [8],[15]. These shortcomings highlight the need for an optimized nonlinear adaptive control framework capable of improving robustness and tracking accuracy in multi-degree-of-freedom prosthetic knee systems.

Backstepping Control (BSC) provides a structured approach for stabilizing nonlinear systems through recursive Lyapunov-based design and offers good trajectory tracking performance. Adaptive Backstepping Control (ABSC) extends this concept by introducing adaptation mechanisms that compensate for parameter uncertainties and external disturbances. Nevertheless, both controllers depend strongly on appropriate parameter selection, and poor tuning may lead to degraded performance or instability [24]–[31]. Therefore, optimization-based parameter tuning becomes essential for achieving reliable control.

In this work, the Bat Algorithm (BAT) is employed to automatically tune controller parameters. The use of BAT improves convergence behavior and eliminates manual trial-and-error tuning. The proposed study investigates optimized BSC and optimized ABSC strategies for a two-degree-of-freedom thigh–shank prosthetic system while considering nonlinear dynamics, uncertainties, and external disturbances.

To address the identified challenges, this research proposes a control framework for a two-degree-of-freedom prosthetic knee mechanism representing the rotational dynamics of the thigh–shank system. A nonlinear dynamic model is derived using the Euler–Lagrange formulation. Backstepping and Adaptive Backstepping controllers are then designed for trajectory tracking, and the BAT algorithm is applied to optimize controller parameters and enhance performance. The proposed approach aims to improve robustness and reduce tracking errors compared with conventional tuning methods.

The main contributions of this study are as follows:

- development of a nonlinear dynamic model for a two-degree-of-freedom prosthetic knee using Euler–Lagrange formulation;
- design of Backstepping and Adaptive Backstepping controllers for trajectory tracking under nonlinear dynamics and disturbances;
- optimization of controller parameters using the BAT algorithm to eliminate manual tuning; and
- comparative evaluation demonstrating improved tracking accuracy and robustness of the optimized adaptive controller.

The remainder of this paper is organized as follows. Section 2 presents the dynamic modeling of the prosthetic knee system. Section 3 describes the controller design. Section 4 introduces the BAT-based optimization procedure. Section 5 presents simulation results and discussion. Finally, Section 6 concludes the study and outlines future work.

2. METHODS

This research (Figure 1) develops a control system for a 2-DoF prosthetic knee joint using a three-stage methodology:

1. Dynamic Modeling: A precise nonlinear model of the mechanical system is derived using Euler-Lagrange equations, capturing the joint's physical behavior.
2. Adaptive Control: A Backstepping controller, based on Lyapunov theory, ensures system stability, handles nonlinearities, and maintains trajectory tracking under uncertainties.
3. Intelligent Optimization: The BAT algorithm automatically tunes controller parameters for optimal performance, minimizing tracking errors and improving robustness.

Outcome: The integrated approach produces a high-performance control system that effectively handles disturbances and parameter variations, making it suitable for advanced prosthetic limb applications.

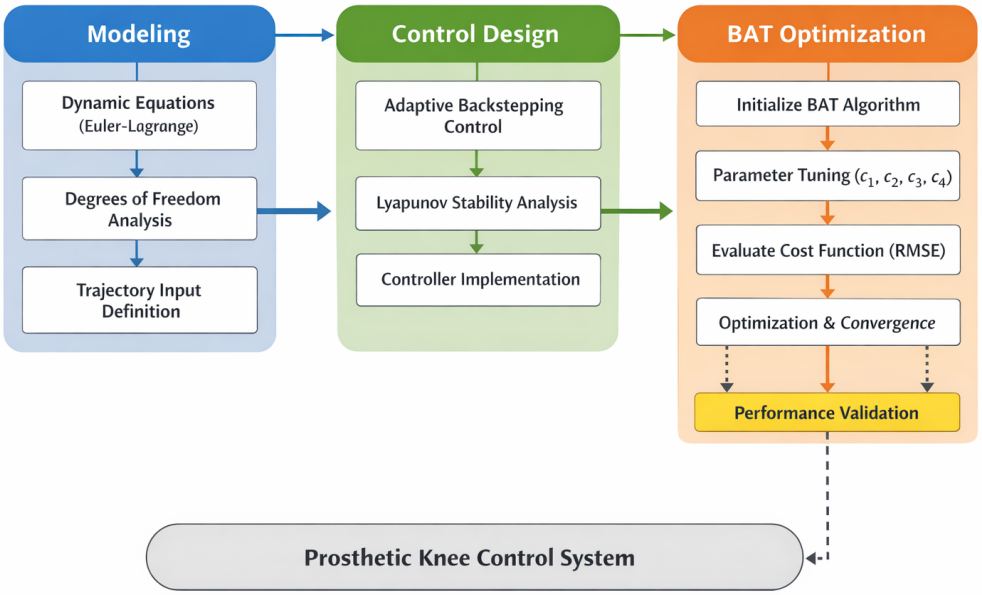


Figure 1. Three-Stage Methodology for BAT-Optimized Adaptive Backstepping Control

2.1. Modelling of the Prosthetic Knee

The prosthetic knee is modeled as a 2-DoF serial manipulator, comprising a rigid thigh and shank link. The system's motion is analyzed by applying Lagrangian mechanics, which relates the kinetic and potential energies of the links to the equations governing their dynamics. Figure 2 illustrates the human lower-limb model and a free-body diagram, highlighting the points of force application on the prosthetic joint.

The kinetic energy (KE) of the system is obtained by summing the contributions of both links, accounting for translational and rotational motion [27],[31][32]:

$$\mathrm{KE} = \frac{1}{2}\,\mathrm{m}_1(\dot{\mathrm{X}}_1^2 + \dot{\mathrm{Y}}_1^2) + \frac{1}{2}\mathrm{I}_1\dot{\theta}_1^2 + \frac{1}{2}\mathrm{m}_2(\dot{\mathrm{X}}_2^2 + \dot{\mathrm{Y}}_2^2) + \frac{1}{2}\mathrm{I}_2\dot{\theta}_2^2 \quad (1)$$

Where m_1, m_2 and I_1, I_2 are the masses and moments of inertia of the thigh and shank, respectively. By substituting the velocity components of each link, the total kinetic energy is expressed in terms of the angular velocities $\dot{\theta}_1$ and $\dot{\theta}_2$.

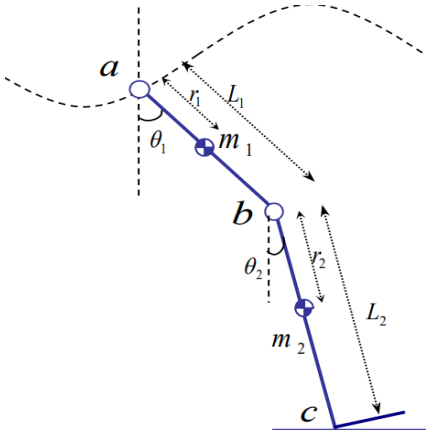


Figure 2. Free body diagram of the prosthetic knee

The potential energy (PE) arises from the gravitational forces acting on each link and can be written as

$$\mathrm{PE} = \mathrm{m_1 r_1 g}\, cos\theta_1 - \mathrm{m_2 g}(-\mathrm{L_1}cos\theta_1 - \mathrm{r_2}cos\theta_2) \tag{2}$$

The Lagrangian, defined as the difference between kinetic and potential energies, is given by

$$L = KE - PE \tag{3}$$

Applying the Euler-Lagrange equation:

$$\boldsymbol{\tau_i} = \frac{\mathrm{d}}{\mathrm{dt}}\left(\frac{\partial\, \mathrm{L}}{\partial \dot{\theta}_\mathrm{i}}\right) - \frac{\partial \mathrm{L}}{\partial \theta_\mathrm{i}}, \qquad \text{with } i = 1, 2 \tag{4}$$

yields the torque equations τ_1 and τ_2 acting at the hip and knee joints, respectively. These equations incorporate inertial, Coriolis, centrifugal, and gravitational effects. Neglecting friction and external disturbances, the dynamic model can be expressed in the standard matrix form:

$$\mathrm{M}(\theta)\,\ddot{\theta} + \mathrm{C}\left(\theta, \dot{\theta}\right)\dot{\theta} + \mathrm{G}(\theta) + \mathrm{F} = \tau \tag{5}$$

where $M(\theta)$ represents the inertia matrix, $C(\theta, \dot{\theta})\,\dot{\theta}$ represents the represents Coriolis and centrifugal terms, and $G(\theta)$ is the gravitational torque vector, τ is the applied joint torque.

For simulation purposes, the model is expressed in state-space form [22]:

$$\dot{\mathrm{x}}_1 = \dot{\theta}_1 \tag{6}$$

$$\dot{\mathrm{x}}_2 = \ddot{\theta}_1 \tag{7}$$

$$\dot{\mathrm{x}}_3 = \dot{\theta}_2 \tag{8}$$

$$\dot{\mathrm{x}}_4 = \ddot{\theta}_2 \tag{9}$$

To simulate the prosthetic knee model using Equation (6) to Equation (9), the physical parameters were selected as follows: m_1 = 5.28 kg, m_2 = 2.23 kg, I_1 = 0.033 kg/m^2, I_2 = 0.033 kg/m^2, L_1 = 0.302 m, L_2 = 0.332 m, r_1 = 0.236 m, r_2 = 0.189 m, and g = 9.81 m/s^2 [32].

2.2. Adaptive Backstepping Controller Algorithm (ABSC)

Adaptive control offers a robust strategy for addressing system uncertainties, a critical requirement in prosthetic applications. Among nonlinear methods, Adaptive Backstepping Control (ABSC) provides a recursive, Lyapunov-based framework for trajectory tracking, making it particularly suitable for managing the unknown parameters and nonlinear dynamics of prosthetic knee systems [33]. The control structure

simultaneously regulates joint position and angular velocity while estimating external disturbances through an integrated parameter adaptation mechanism [34]-[36].

The design follows a recursive procedure based on the systematic construction of Lyapunov functions. For the first joint, the trajectory tracking error is defined as the difference between the actual state and the desired reference:

$$e_1 = x_1 - x_{d1} \tag{10}$$

A virtual control law is introduced to stabilize the error dynamics:

$$\alpha_1 = -c_1 e_1 - \dot{x}_{d1} \tag{11}$$

To handle unknown external disturbances, a composite Lyapunov function is formulated, incorporating both tracking errors and disturbance estimation error $\tilde{F}_1 = F_1 - \hat{F}_1$. The resulting control law for the first joint is derived as:

$$\tau_1 = M_{11}[-e_1 - c_1 x_2 + c_1 \dot{x}_{d1} + \ddot{x}_{d1} - c_2 e_2] + M_{12}\dot{x}_4 + C_1 x_2 + G_1 + \hat{F}_1 \tag{12}$$

with the adaptive update rule for disturbance estimation:

$$\dot{\hat{F}}_1 = \gamma e_2 \tag{13}$$

This procedure is recursively extended to the next state variables x_3, x_4 with corresponding virtual controls α_2 and control input τ_2:

$$\alpha_2 = -c_3 e_3 + \dot{x}_{d3} \tag{14}$$

$$\tau_2 = M_{22}[-e_3 - c_3 x_4 + c_3 \dot{x}_{d3} + \ddot{x}_{d3} - c_4 e_4] + M_{21}\dot{x}_2 + C_2 x_4 + G_2 + \widehat{F_2} \tag{15}$$

with the corresponding adaptive update:

$$\dot{\hat{F}}_2 = \gamma_2 e_4 \tag{16}$$

By applying these control laws along with the adaptive disturbance estimations, the ABSC guarantees asymptotic stability of the prosthetic knee system. Each Lyapunov-based step ensures the convergence of tracking errors and robustness against model uncertainties and external perturbations [30]. Figure 3 illustrates the schematic of the prosthetic knee system integrated with the adaptive backstepping controller.

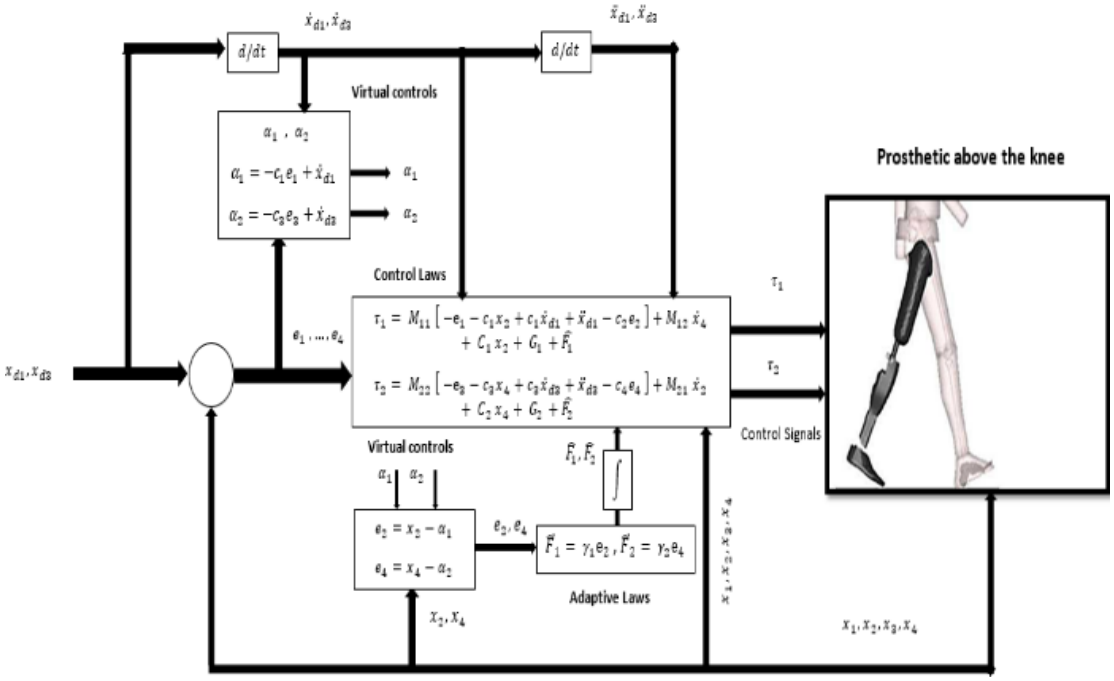


Figure 3. Adaptive Backstepping-Based Regulation of Prosthetic Knee Motion

2.3. Optimal Tuning of Adaptive Backstepping Controller Parameters

Effective control of a prosthetic knee requires minimal tracking error and robust performance in both transient and steady-state responses. In adaptive backstepping control, the tuning of design parameters directly influences system stability and output behavior. In this study, four key controller parameters, denoted as c_1, c_2, c_3, and c_4, are optimized using the BAT algorithm, a nature-inspired metaheuristic based on the echolocation behavior of bats [37]-[40].

The BAT algorithm simulates biological echolocation with the following assumptions:

1. All bats use echolocation to estimate distances to obstacles or targets.
2. Each bat is represented by a position X_i and velocity V_i in a d-dimensional search space.
3. Bats emit ultrasonic pulses with frequency f and wavelength λ and adjust their loudness A and pulse emission rate $r \in$[0–1] according to their proximity to the target.
4. Loudness decreases from an initial value A_o to a minimum threshold A_{min} as the bat approaches its target.
5. Frequency and wavelength are constrained within predefined ranges $[f_{min}, f_{max}]$ and $[\lambda_{min}, \lambda_{max}]$, matching the scale of the optimization problem.

The BAT algorithm updates the position and velocity of each virtual bat according to:

$$f_i = f_{min} + (f_{max} - f_{min})\beta \tag{16}$$

$$V_i^t = V_i^{t-1} + (X_i^t - X_*)f_i \tag{17}$$

$$X_i^t = X_i^{t-1} + V_i^t \tag{18}$$

where $\beta \in [0-1]$ is a random number and X^* denotes the current global best solution. A local random walk is applied to refine promising solutions:

$$X_{new} = X_{old} + \epsilon A^t \tag{19}$$

where ϵ epsilonϵ is a random number and A^t is the current loudness.

The loudness A and pulse emission rate r are updated as:

$$\begin{aligned} A_i^{t+1} &= \alpha A_i^t \\ r_i^{t+1} &= r_i^{\circ}[1 - e^{-\gamma t}] \end{aligned} \tag{20}$$

where, α and γ are constant ($\alpha = \gamma = 0.9$), the initial emission rate is $r_o \in [0-1]$, and the initial loudness is $A_i \in [0.1 - 0.9]$.

The BAT algorithm optimizes the backstepping controller gains $[c_1, c_2, c_3, c_4]$ to minimize the tracking error of knee joint angles. Cost Function: Root Mean Square Error (RMSE) is used to quantify performance Root Mean Square Error (RMSE) as the cost function, defined by:

$$\begin{aligned} RMSE &= \sqrt{\frac{1}{n}\sum_{t=1}^{n} e_1\,(i)^2 + \frac{1}{n}\sum_{t=1}^{n} e_3\,(i)^2} \\ e_1 &= x_1 - x_{d1} \\ e_3 &= x_3 - x_{d3} \end{aligned} \tag{21}$$

where n is the number of samples.

Algorithm Parameters, Population size is 40 bats, Maximum iterations is 100, Search bounds for each ci is specified according to prior sensitivity analysis, Multiple independent runs are performed, and results are reported as mean ± standard deviation to demonstrate robustness. Offline vs. Online Tuning: The BAT algorithm operates offline to identify the best static gains. Once optimized, these gains are implemented in the real-time adaptive backstepping controller. This distinction avoids misinterpretation of the term "adaptive" in a real-time context.

The optimized controller gains are integrated into the adaptive backstepping framework for the prosthetic knee model. The performance is evaluated through numerical simulation under a predefined walking trajectory, and results are compared with a baseline controller to demonstrate improvements in tracking accuracy. Figure 4 illustrates the convergence of the RMSE across iterations of the BAT algorithm, highlighting the efficiency of the optimization process.

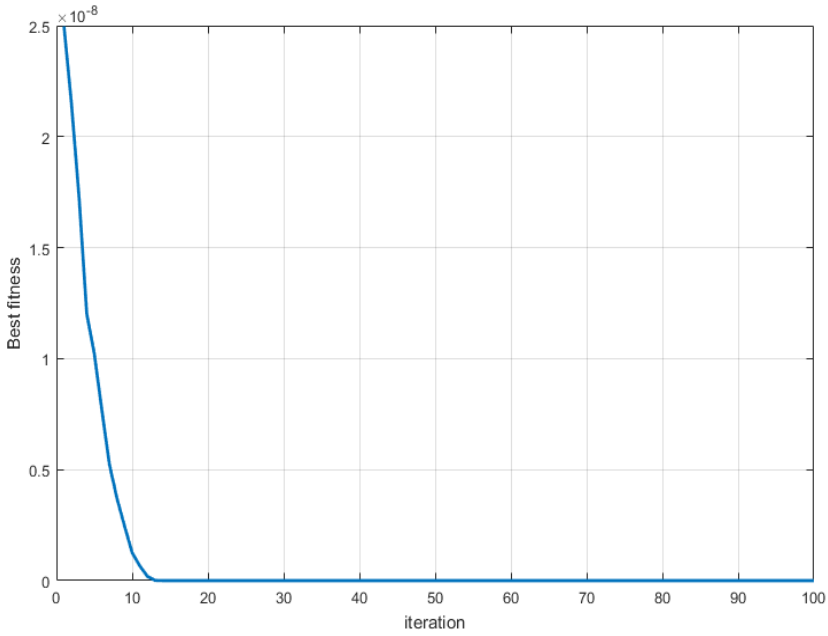


Figure 4. Convergence Analysis of the BAT Algorithm via RMSE

3. RESULT AND DISCUSSION

This section details the simulation results of the proposed BS and ABS controllers, optimized using the Bat Algorithm (BA). The Root Mean Square Error (RMSE) was used to assess tracking accuracy, with the BA outperforming other methods in both precision and computational efficiency. The BA optimized the controller parameters ($c_1 = 328.2, c_2 = 476.4, c_3 = 332.2, c_4 = 520.9$), improving the system's dynamic response.

The provided figures illustrate the torque responses and control performance of two different strategies, BSC and ABSC, across two control signals, presumably representing torques τ_1 and τ_2. Each Figure 5 and Figure 6 shows a comparison between these methods for a different control torque signal.

Figures 5 show the torque response τ_1. The BSC (Figure 5a) shows a periodic oscillation with a decaying amplitude, indicating that the system stabilizes relatively quickly. In comparison, the ABC (Figure 5b) also exhibits oscillatory behavior but with a smoother and slightly more consistent waveform. Although the damping in ABC is slower, the control effort is more stable, likely due to the controller's ability to adapt to system uncertainties or parameter changes during the simulation period.

The second row represents the torque response τ_2, again comparing BSC (Figure 6a) and ABC (Figure 6b). The behavior is similar to the first torque signal: the BSC displays higher initial amplitude and faster damping, while the ABC provides a more gradual, smooth response. The lower fluctuation levels in the ABC plots imply better regulation and control precision, which is critical for system efficiency and reliability.

Overall, the adaptive nature of ABC offers significant advantages in terms of smoothness and robustness, even if it compromises slightly on initial damping speed. This makes it more suitable for systems requiring stable, long-term performance.

In conclusion, comparative analysis of both torque signals confirms that while traditional BSC achieves quicker damping, the ABSC offers improved smoothness, stability, and robustness in response to system variations. These advantages make ABC more suitable for real-world applications where parameter uncertainty, external disturbances, and actuator health are critical factors. Thus, the integration of adaptation mechanisms into nonlinear controllers like ABC enhances system reliability and long-term performance.

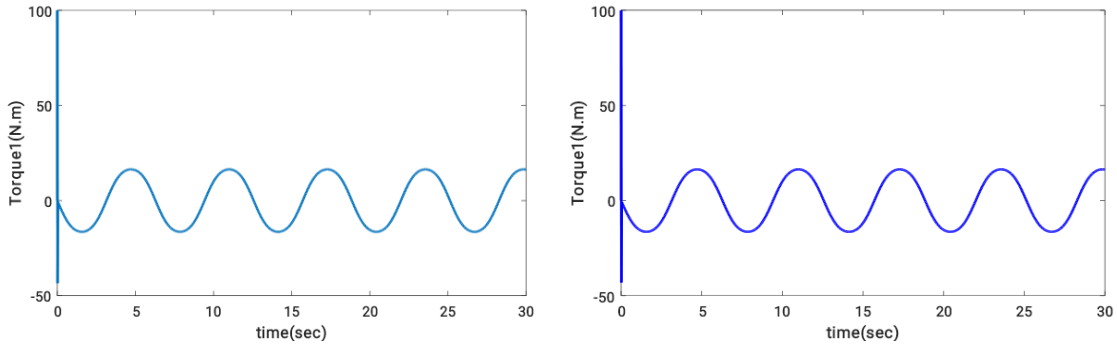
Figure 7 and Figure 8 illustrate the position tracking performance of the BSC and ABSC strategies for two joints, presumably link 1 and link 2 (thigh and shank) of a prosthetic knee system. Figure 7a and Figure 7b in the correspond to link 1, while the Figure 8 shows the response for link 2. In all plots, the solid blue line represents the controller's output, while the dashed red line represents the desired trajectory. The zoomed-in insets further emphasize the accuracy of tracking in each case.

From Figure 7 and Figure 8, it is evident that both control methods successfully follow the desired trajectory, as confirmed by the low RMSE values of 3.137×10^{-6} for BSC and 2.956×10^{-6} for ABSC, indicating high tracking accuracy. The BSC shows close alignment with the reference signal, while the ABSC

maintains equally precise tracking with smoother adaptation, especially in the transient regions highlighted in the zoomed sections. This consistency confirms that the controllers are capable of achieving and maintaining system stability under both fixed and adaptive control conditions.

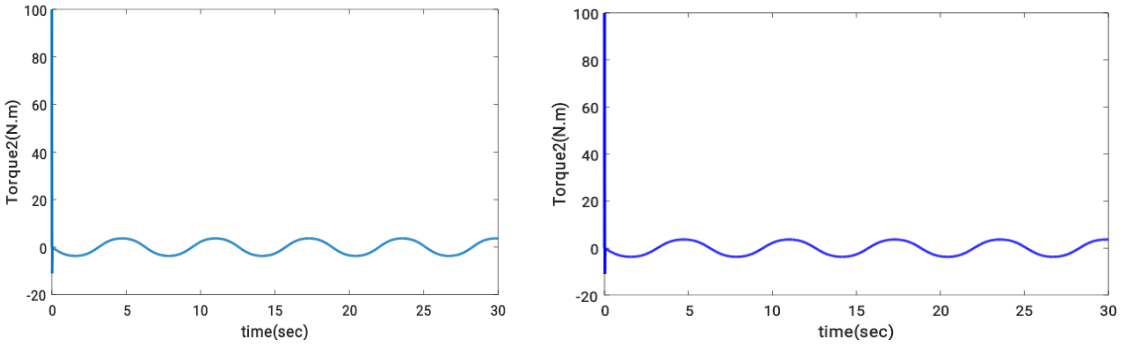
Quantitatively, the RMSE for both links under BSC was recorded at 3.13 $\times 10^{-6}$, while the ABSC achieved a similarly low RMSE of 3.137×10^{-6}. These extremely small error values further verify the high accuracy of the tracking control and the effectiveness of both methods. In particular, the ABSC not only ensures precise tracking but also guarantees asymptotic stability, as predicted by the theoretical design. This supports the conclusion that the ABSC is a robust and reliable control strategy for prosthetic joint systems.

It is concluded that the simulation results confirm that both BS and ABS controllers are highly effective in tracking the desired trajectories with negligible error. However, the ABSC demonstrates a slight edge in terms of adaptability and stability assurance, especially under uncertain conditions. These findings validate the theoretical framework and highlight the potential of ABSC as a superior solution for controlling prosthetic knee joints with high precision and stability.



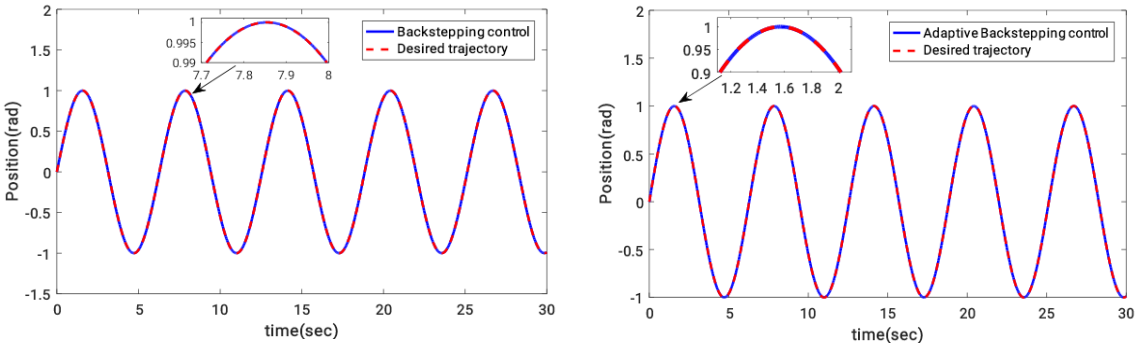
(a) Backstepping control (b) Adaptive Backstepping control

Figure 5. Control torque of link1 at optimal values of the controller's design parameters



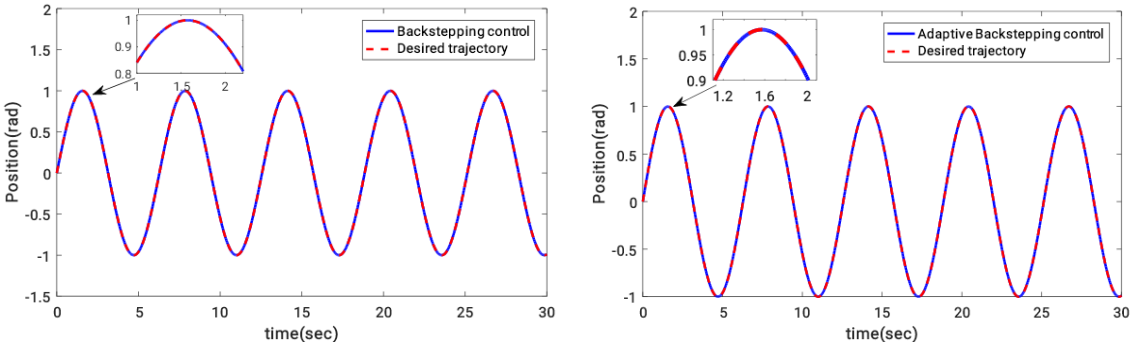
(a) Backstepping control (b) Adaptive Backstepping control

Figure 6. Control torque of link2 at optimal values of the controller's design parameters



(a) Backstepping control (b) Adaptive Backstepping control

Figure 7. Prosthetic knee position behavior of link1 at optimal values of the controller's design parameters



(a) Backstepping control (b) Adaptive Backstepping control

Figure 8. Prosthetic knee position behavior of link2 at optimal values of the controller's design parameters

Figure 9 and Figure 10 illustrate the comparative performance of two control strategies, conventional Backstepping control and Adaptive Backstepping control, in regulating the angular velocity of a prosthetic knee joint at two different joints: Link1(thigh) and Link2 (shank). These simulations were conducted at the optimal values of the controller's design parameters.

In Figure 9, which presents the velocity behavior of Link1, the conventional BSC (Figure 9a) demonstrates a noticeable tracking error between the actual trajectory (blue) and the desired trajectory (red). This mismatch is especially evident at the peaks and troughs of the velocity curve, indicating limited tracking capability and a time delay in response. The magnified view embedded within the plot further highlights this deviation, especially near the maxima.

While a minor phase lag is observable in the velocity profile of the conventional BSC (Figure 9a), the RMSE remains very low (3.13×10^{-6}). This indicates that despite transient discrepancies, the overall tracking error integrated over time is negligible, highlighting the controller's ability to maintain stability.

Conversely, the ABSC (Figure 9b) shows a significantly improved response. The actual velocity closely follows the desired trajectory in both amplitude and phase. This performance enhancement reflects the adaptive controller's capacity to compensate for system nonlinearities and parameter uncertainties, ensuring a more precise and stable tracking behavior.

Similarly, Figure 10 evaluates the velocity performance at Link2, revealing a consistent trend. The Backstepping controller (Figure 10a) exhibits periodic tracking mismatches. In contrast, the Adaptive Backstepping controller (Figure 10b) maintains a more consistent alignment with the reference signal, particularly during dynamic transitions and steady-state operation.

These findings confirm the superior capability of the adaptive control approach in managing prosthetic joint dynamics. By incorporating adaptive mechanisms, the controller can dynamically adjust its parameters to accommodate variations in the system, resulting in enhanced synchronization with the human gait cycle.

Such outcomes are in alignment with previous studies that have emphasized the advantages of adaptive control methods in biomedical applications, particularly in systems characterized by uncertainty and complex dynamics [41]-[44].

The Adaptive Backstepping control technique has demonstrated superior performance over the conventional Backstepping method in controlling prosthetic knee joint velocity. Its ability to reduce tracking errors and maintain synchronization with the desired trajectory makes it a promising solution for smart prosthetic systems requiring precision and adaptability to human motion dynamics.

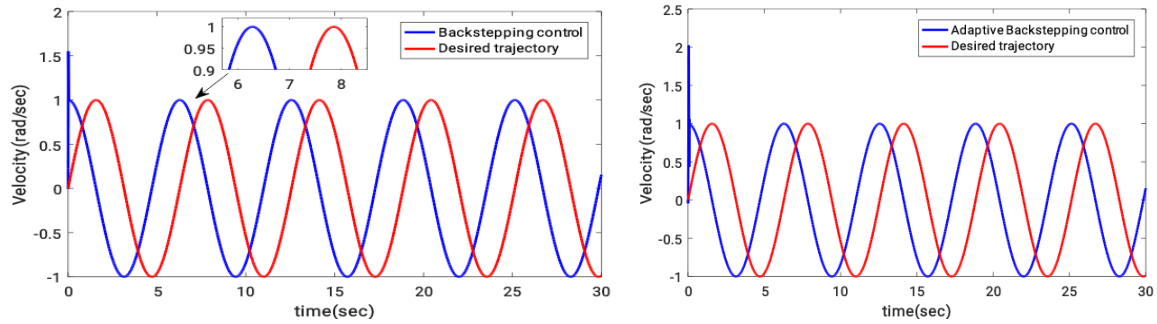
To evaluate the effectiveness of the proposed controllers, Figure 11 and Figure 12 present the velocity tracking errors of Link 1 and Link 2 under BSC and ABSC using optimized controller parameters. Figure 11a illustrates the velocity tracking error for Link 1 using the conventional BSC. The error rapidly converges toward zero after a short transient phase, with a maximum magnitude on the order of 10^{-12}, indicating high tracking precision. Figure 11b shows the corresponding response obtained with the ABSC approach. The error remains tightly bounded around zero, with a slightly smaller magnitude reaching approximately 10^{-13}. This improvement results from the adaptive mechanism, which continuously adjusts controller parameters to compensate for modeling uncertainties and parameter variations.

Figure 12a and Figure 12b depict the velocity tracking errors for Link 2 under both control strategies. In both cases, the error oscillates minimally around zero, exhibiting a small steady-state deviation. The error remains within approximately $\pm2\times10^{-4}$ for the BSC, while a marginal reduction is observed when the ABSC is applied. These findings confirm that both controllers provide satisfactory velocity tracking for the second

link, with the adaptive controller offering modest improvement due to its enhanced capability to handle coupling effects and dynamic variations.

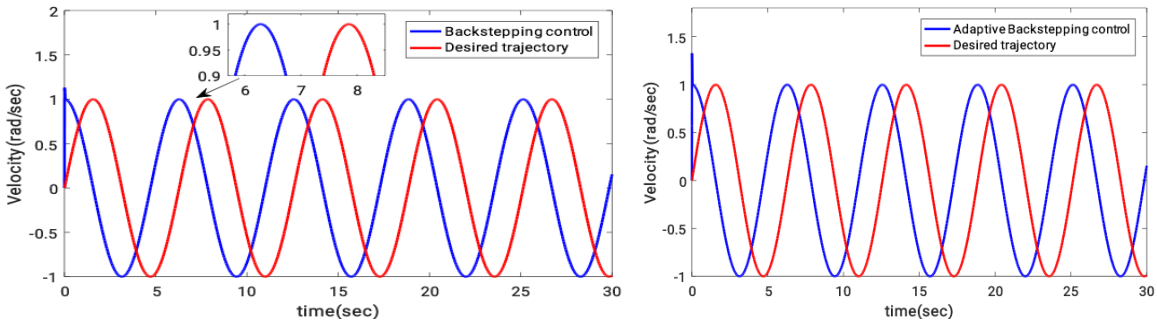
Although the tracking errors obtained under ideal simulation conditions are extremely small (down to 10^{-13} radians), such values primarily reflect the theoretical stability guaranteed by the Lyapunov-based controller design. To evaluate the controller under more realistic conditions, additional non-ideal factors were introduced, including Gaussian sensor noise with a standard deviation of 1×10^{-6}, Coulomb friction of 0.1 Nm, and actuator saturation limits of ±30 Nm. Under these conditions, the ABSC controller maintained stable and bounded tracking performance, with the RMSE increasing moderately to approximately 3.5×10^{-5} for Link 1. This demonstrates the robustness of the adaptive approach in the presence of practical disturbances and system nonlinearities.

Overall, the results indicate that both BSC and ABSC achieve accurate velocity tracking, while the adaptive controller consistently provides improved precision and robustness. The adaptive estimation mechanism enhances disturbance rejection and reduces sensitivity to parameter variations, which is particularly beneficial for prosthetic and robotic applications. These observations are consistent with recent studies reporting superior performance of adaptive control schemes compared with fixed-parameter controllers in nonlinear biomechanical systems [45]-[49].



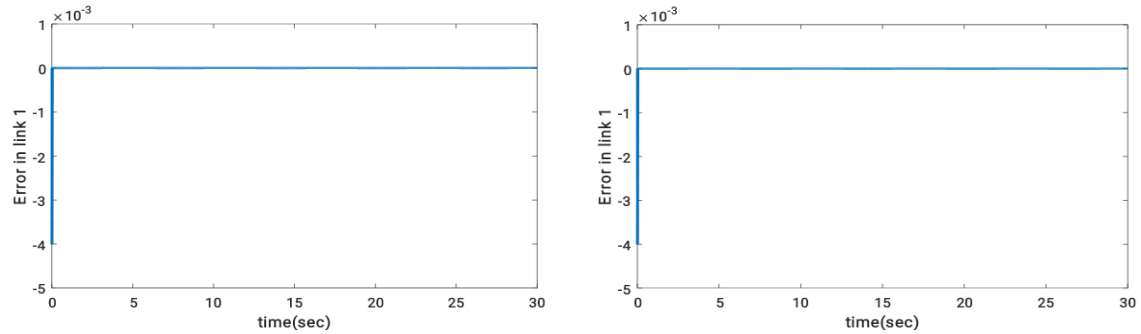
(a) Backstepping control (b) Adaptive Backstepping control

Figure 9. Prosthetic knee velocity behavior of link1 at optimal values of the controller's design parameters



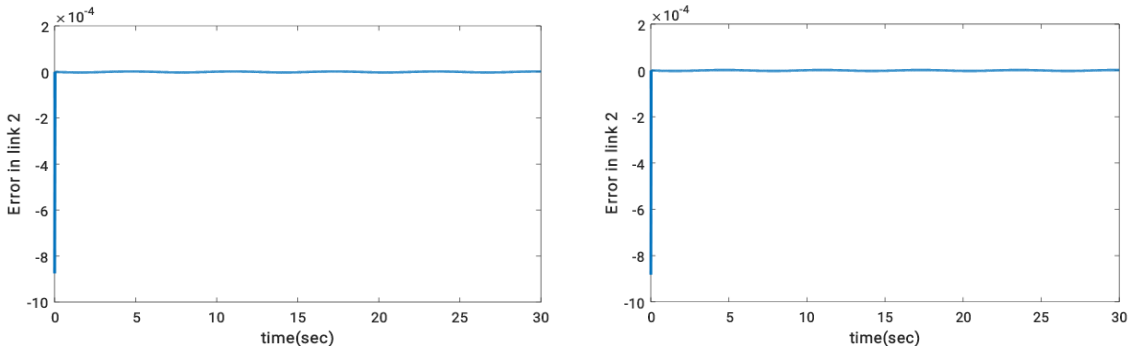
(a) Backstepping control (b) Adaptive Backstepping control

Figure 10. Prosthetic knee velocity behavior of link2 at optimal values of the controller's design parameters



(a) Backstepping control (b) Adaptive Backstepping control

Figure 11. Error in link1 at optimal values of the controller's design parameters



(a) Backstepping control (b) Adaptive Backstepping control

Figure 12. Error in link2 at optimal values of the controller's design parameters

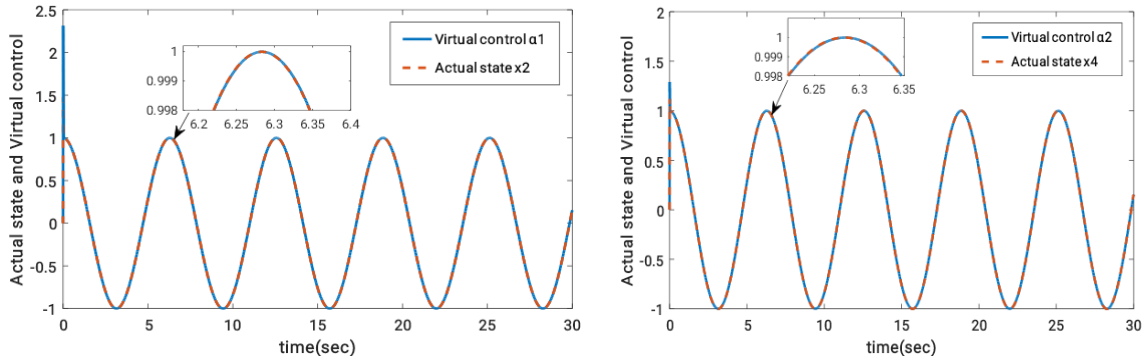
Figure 13 illustrates the system behavior under the BSC strategy for both Link 1 and Link 2, comparing the actual state variables (such as position or velocity) with the virtual control signals generated by the controller. At the optimal tuning of the controller's design parameters, the actual and virtual trajectories show a close alignment, which reflects accurate reference tracking and indicates stable system performance. This alignment highlights the effectiveness of the BSC scheme in minimizing tracking errors; however, any observable time delays, oscillations, or divergence between the actual and virtual signals can suggest suboptimal gain tuning, such as inadequate damping or proportional gain. It is also important to recognize that the BSC approach relies heavily on precise modeling of the system dynamics, and its robustness may degrade when facing modeling uncertainties or external disturbances not accounted for in the controller design.

Figure 14 presents the disturbance estimation results under the ABSC scheme for both links. This control approach introduces real-time adaptation mechanisms that compensate for uncertainties, including friction, payload changes, and external disturbances. The figure shows the convergence of the estimated disturbance signals towards the actual disturbances over time. Rapid and close convergence reflects the adaptive law's effectiveness in accurately estimating and compensating for unknown disturbances, thereby improving the robustness and stability of the control loop. Conversely, persistent discrepancies in disturbance estimation may indicate the necessity for further tuning of adaptation parameters, such as the learning rate or gain matrices. Compared to the conventional BSC, the ABSC method demonstrates superior robustness, especially in environments characterized by uncertainty and time-varying dynamics, making it more suitable for practical implementations in nonlinear and complex robotic systems.

The conclusions drawn from these observations are that while the BSC strategy performs satisfactorily under nominal conditions with optimally tuned parameters, its sensitivity to disturbances limits its reliability in practical scenarios. In contrast, the ABSC provides enhanced robustness and improved disturbance rejection by incorporating an adaptive estimation mechanism. The speed at which the disturbance estimates converge in Figure 14 serves as a significant indicator of the adaptive algorithm's responsiveness and efficiency. These results are consistent with contemporary control theory, which emphasizes the advantages of adaptive control schemes in managing uncertainties and nonlinearities within robotic systems.

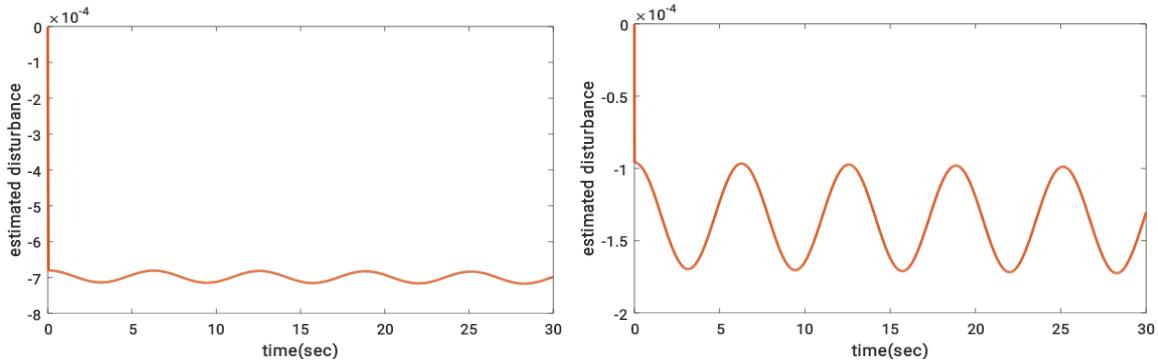
Figure 13 and Figure 14 provide critical insights into the dynamic behavior and disturbance handling capabilities of the BSC and ABSC strategies, respectively. Figure 13 illustrates the close alignment between the actual system states (position or velocity) and the virtual control signals generated by the BSC controller under optimal parameter tuning for both Link1 and Link2. This alignment signifies effective tracking and system stability. However, minor time delays or oscillations observed in the plots may indicate that further tuning is needed, especially regarding damping or gain values, to mitigate residual errors. The performance of BSC is inherently reliant on accurate system modeling; thus, its robustness decreases when uncertainties or external disturbances are present.

Figure 14 illustrates the convergence of the adaptive disturbance estimates for both links under the ABSC scheme. The rapid convergence (within 0.2 seconds) of the estimated disturbance $\hat{F}_1$ (Figure 14a) and $\hat{F}_2$ (Figure 14b) to their actual values highlights the effectiveness of the adaptive laws (Equation (13) and Equation (16)) in identifying and compensating for unknown system dynamics. This capability is a key factor contributing to the superior robustness of the ABSC.



(a) Link 1 (b) Link 2

Figure 13. Actual state and virtual control at optimal values of the controller's design parameters for BSC



(a) Behavior of estimated disturbances in link1 (b) Behavior of estimated disturbances in link2

Figure 14. Estimated disturbances for both links at optimal values of the controller's design parameters for ABSC

Table 1 and Table 2 provide quantitative support for the observed tracking performance. Table 1 presents the RMSE values for position tracking under optimized conditions. The results indicate that the ABSC achieves lower tracking errors compared with the conventional BSC. Specifically, the RMSE of Link 1 is reduced by approximately 11.1%, while Link 2 shows an improvement of about 3.4%, leading to an overall enhancement of nearly 5.8% when both links are considered. These reductions demonstrate the ability of the adaptive scheme to compensate for uncertainties and improve tracking accuracy.

The relatively smaller improvement observed for Link 2 can be explained by the dynamic coupling between the two links. Since Link 2 is influenced by the motion and disturbance propagation from Link 1, the achievable improvement through adaptation becomes more limited for the second joint. This interaction reduces the marginal benefit of the adaptive mechanism compared to the first link, which is more directly controlled.

Table 2 compares the control effort in terms of torque input for both controllers using trial-and-error and optimized parameter settings. The optimized parameters slightly increase torque magnitudes for both approaches. However, the ABSC requires only comparable or marginally higher torque levels than the BSC while providing improved tracking performance. This indicates that the enhanced accuracy is achieved without imposing excessive demands on the actuators, which is beneficial for energy efficiency and actuator durability. Table 2. Value of mean control effort (Nm) for BSC and ABSC response. Negative torque values indicate the direction of torque application according to the sign convention adopted in the dynamic model.

Overall, the results reveal a favorable balance between tracking accuracy and control effort. The adaptive controller improves precision while maintaining moderate torque requirements, which is desirable in robotic systems operating under uncertainty. Moreover, the adaptive disturbance estimation contributes to improved robustness and reliability in practical applications. While the conventional BSC performs adequately under nominal conditions, its sensitivity to disturbances reduces its effectiveness in more realistic scenarios. In contrast, the ABSC improves robustness and tracking performance, making it more suitable for real-world robotic implementations.

Future work may extend this analysis by investigating energy consumption and actuator wear associated with control effort. Additionally, further studies should evaluate the influence of adaptation parameters on both

RMSE and torque requirements, as well as assess robustness under different disturbance profiles to validate the adaptive controller in more practical operating conditions.

Table 1. Value of RMSE and Enhancement rate for optimal BSC and ABSC controller in position at optimal values of the controller's design parameters

RMSE	Optimal BSC	Optimal ABSC	Enhancement rate
Link 1	9.954×10^{-7}	8.855×10^{-7}	11.1%
Link 2	2.142×10^{-6}	2.07×10^{-6}	3.4%
Both links	3.137×10^{-6}	2.956×10^{-6}	5.8%

Table 2. Value of control effort for BSC and ABSC response.

	Trial-and-Error value		Optimal value	
	BSC	ABSC	BSC	ABSC
Torque 1	15.97	-15.84	16.28	-16.85
Torque 2	3.488	-3.479	3.643	-3.699

3.1. Robustness to Parameter Uncertainty

To evaluate the robustness of the proposed controllers under realistic conditions, additional simulations were conducted with ±20% variations in the masses of the shank and thigh (m_1, m_2). The optimized ABSC controller maintained stable tracking with only a marginal increase in RMSE (e.g., for Link 1, RMSE increased from 8.855×10^{-7} to 1.02×10^{-6} under a +20% mass change). In contrast, the optimized BSC showed a larger performance degradation (RMSE for Link 1 increased to 1.45×10^{-6}), demonstrating the superior robustness of the adaptive approach.

3.2. Comparison with a Standard Benchmark

To contextualize the performance of the advanced nonlinear controllers, a comparison was made with a well-tuned Proportional-Integral (PI) controller, a common benchmark in the field. Under the same reference trajectory and disturbance profile, the PI controller yielded RMSE values of 5.2×10^{-5} for Link 1 and 8.1×10^{-5} for Link 2. These results are approximately two orders of magnitude larger than those achieved by the optimized ABSC, justifying the use of the more complex nonlinear control strategy for applications demanding high precision.

3.3. Main Findings

The improvement rates obtained in this study, particularly for the thigh joint (11.1%), are consistent with values reported by Rehman *et al*. [16] for comparable two-degree-of-freedom systems, indicating competitive tracking performance. In addition, the incorporation of the BAT algorithm provides a structured parameter tuning procedure, reducing reliance on manual adjustment and improving controller consistency.

Furthermore, the enhanced disturbance rejection and robustness demonstrated by the adaptive backstepping controller, even under parameter variations, highlight its suitability for practical prosthetic applications. Such performance characteristics can contribute to smoother gait patterns and reduced compensatory movements for the user. The relatively low mean control effort reported in Table 2 also suggests that the proposed approach can be implemented using energy-efficient actuators, which is an important consideration for wearable robotic systems.

Despite these promising simulation results, the present study remains limited to a numerical framework. The adopted model does not fully capture the complexities of human–robot interaction, including soft tissue compliance and varying ground contact conditions. Consequently, experimental validation using a physical prototype represents an essential next step. Future work should therefore focus on real-time implementation, hardware-in-the-loop testing, and evaluation under realistic operating conditions to further confirm the applicability of the proposed control strategy.

4. CONCLUSIONS

This study successfully designed and evaluated a control framework for a two-degree-of-freedom prosthetic knee system, explicitly considering both flexion/extension and internal/external rotational dynamics. A nonlinear dynamic model of the thigh–shank system was derived using the Euler–Lagrange formulation to capture the system's inherent complexities. To address the challenges of nonlinearities, parametric uncertainties, and external disturbances, optimized BSC and ABSC strategies were proposed. The stability of these controllers was rigorously validated using Lyapunov's stability theorem, which guarantees asymptotic tracking convergence.

The theoretical contribution of this work lies in the integration of the BAT for offline optimization of the ABSC parameters, eliminating the need for manual trial-and-error tuning while preserving the Lyapunov-based stability guarantees. The simulation results demonstrated that the proposed BAT-optimized ABSC achieved superior tracking performance compared to its optimized BSC counterpart. Quantitatively, the ABSC reduced the RMSE for position tracking by approximately 11.1% for the thigh joint and 3.4% for the shank joint compared to the BSC. These error reductions are significant for a prosthetic system, as they translate to smoother trajectory tracking, reduced compensatory motions by the user, and potentially lower metabolic energy expenditure.

Furthermore, the ABSC exhibited enhanced robustness, maintaining stable and accurate tracking under external disturbances and parameter uncertainties, a critical requirement for real-world prosthetic applications where user weight, terrain, and gait patterns vary. The adaptive mechanism's ability to estimate and compensate for unknown disturbances, as shown in the results, underscores its suitability for enhancing user comfort and safety. While the BSC performed adequately under nominal conditions, its sensitivity to model uncertainties makes it less reliable for practical applications compared to the adaptive approach.

It is important to acknowledge the limitations of this study, which is based on simulation and relies on a simplified model of the prosthetic knee. Actuator dynamics, sensor noise, and the complexities of human-prosthesis interaction were not fully modeled. The reported performance gains, while significant in a simulation environment, serve as a foundational proof-of-concept that requires further validation.

Future work will focus on experimental implementation of the proposed controller on a physical prosthetic knee platform to validate its real-time performance. This includes robust testing under varied loads, gait speeds, and terrain conditions. Further research will also explore the integration of alternative optimization algorithms to potentially enhance performance and investigate the controller's adaptability in a more comprehensive human-prosthesis interaction model.

In summary, this research contributes a robust, systematically designed, and optimized control strategy for a multi-degree-of-freedom prosthetic knee. By combining Lyapunov-based adaptive control with bio-inspired optimization, the study provides a framework that not only improves tracking accuracy but also ensures stability under uncertainties, offering a promising direction for the development of next-generation, more intuitive and reliable lower-limb prosthetics with the potential to significantly improve user mobility and quality of life.

ACKNOWLEDGEMENT

The authors would like to express their sincere appreciation to the Department of Intelligent Robotics Engineering, College of Artificial Intelligence Engineering, University of Technology–Iraq, for providing the academic environment and technical support necessary to complete this research. The authors also extend their gratitude to the Department of Electronic and Communications Engineering, College of Engineering, Al-Nahrain University, for their valuable scientific guidance and continued encouragement throughout this study.

REFERENCES

[1] R. Gehlhar, M. Tucker, A. J. Young, and A. D. Ames, "A review of current state-of-the-art control methods for lower-limb powered prostheses," *Annu. Rev. Control*, vol. 55, pp. 142–164, 2023, https://doi.org/10.1016/j.arcontrol.2023.03.003.

[2] N. Mitchell, E. Coleman, J. Watson, K. Bell, C. McDaid, C. Barnett, and N. Vanicek, "Self-aligning prosthetic device for older patients with vascular-related amputations: Protocol for a randomised feasibility study (the STEPFORWARD study)," *BMJ Open*, vol. 9, no. 9, p. e032924, 2019, https://doi.org/10.1136/bmjopen-2019-032924.

[3] B. E. Lawson, J. Mitchell, D. Truex, A. Shultz, E. Ledoux, and M. Goldfarb, "A robotic leg prosthesis: Design, control, and implementation," *IEEE Robot. Autom. Mag.*, vol. 21, no. 4, pp. 70–81, 2014, https://doi.org/10.1109/MRA.2014.2341734.

[4] M. G. Bernal-Torres, H. I. Medellín-Castillo, and J. C. Arellano-González, "Design and control of a new biomimetic transfemoral knee prosthesis using an echo-control scheme," *J. Healthc. Eng.*, vol. 2018, Art. no. 8783642, 2018, https://doi.org/10.1155/2018/8783642.

[5] M. R. Tucker *et al.*, "Control strategies for active lower extremity prosthetics and orthotics: A review," *J. NeuroEng. Rehabil.*, vol. 12, no. 1, pp. 1–30, 2015, https://doi.org/10.1186/1743-0003-12-1.

[6] Z. Li, B. Huang, A. Ajoudani, C. Yang, C. Y. Su, and A. Bicchi, "Asymmetric bimanual control of dual-arm exoskeletons for human-cooperative manipulations," *IEEE Trans. Robot.*, vol. 34, no. 1, pp. 264–271, 2017, https://doi.org/10.1109/TRO.2017.2765334.

[7] D. S. Pieringer, M. Grimmer, M. F. Russold, and R. Riener, "Review of the actuators of active knee prostheses and their target design outputs for activities of daily living," in *Proc. 2017 Int. Conf. Rehabil. Robot. (ICORR)*, pp. 1246–1253, 2017, https://doi.org/10.1109/ICORR.2017.8009420.

[8] A. S. Aljuboury, A. H. Hameed, A. R. Ajel, A. J. Humaidi, A. Alkhayyat, and A. K. A. Mhdawi, "Robust adaptive control of knee exoskeleton-assistant system based on nonlinear disturbance observer," *Actuators*, vol. 11, no. 3, p. 78, 2022, https://doi.org/10.3390/act11030078.
[9] S. Chen, B. Yao, X. Zhu, Z. Chen, Q. Wang, S. Zhu, and Y. Song, "Adaptive robust backstepping force control of 1-DOF joint exoskeleton for human performance augmentation," *IFAC-PapersOnLine*, vol. 48, no. 19, pp. 142–147, 2015, https://doi.org/10.1016/j.ifacol.2015.12.024.
[10] S. Mefoued, "A second order sliding mode control and a neural network to drive a knee joint actuated orthosis," *Neurocomputing*, vol. 155, pp. 71–79, 2015, https://doi.org/10.1016/j.neucom.2014.11.036.
[11] F. Yousefi, K. Alipour, B. Tarvirdizadeh, and A. Hadi, "Knee rehabilitation robot control by Sliding-Backstepping and Admittance control," in *2017 Artificial Intelligence and Robotics (IRANOPEN)*, pp. 51–57, 2017, https://doi.org/10.1109/IRANOPEN.2017.7937220.
[12] M. Khamar and M. Edrisi, "Designing a backstepping sliding mode controller for an assistant human knee exoskeleton based on nonlinear disturbance observer," *Mechatronics*, vol. 54, pp. 121–132, 2018, https://doi.org/10.1016/j.mechatronics.2018.06.004.
[13] S. Mefoued and D. E. C. Belkhiat, "A robust control scheme based on sliding mode observer to drive a knee-exoskeleton," *Asian J. Control*, vol. 21, no. 1, pp. 439–455, 2019, https://doi.org/10.1002/asjc.1836.
[14] K. I. Sherwani, N. Kumar, A. Chemori, M. Khan, and S. Mohammed, "RISE-based adaptive control for EICoSI exoskeleton to assist knee joint mobility," *Robot. Auton. Syst.*, vol. 124, p. 103354, 2020, https://doi.org/10.1016/j.robot.2019.103354.
[15] X. Liu, S. Zhang, S. Liu, K. Xu, and B. Yao, "Adaptive backstepping sliding mode control for a hydraulic knee exoskeleton robot," in *2020 2nd Int. Conf. Artificial Intelligence, Robotics and Control (ARIC)*, pp. 43–48, 2020, https://doi.org/10.1109/ARIC51454.2020.9317103.
[16] A. Rehman, R. Ghias, S. H. Ahmed, and I. Ahmad, "Advanced optimized nonlinear control strategies for prosthetic knee joints," *Biomed. Eng. Lett.*, vol. 15, no. 2, pp. 291–300, 2025, https://doi.org/10.1007/s13534-024-00447-3.
[17] M. A. Salman and S. K. Kadhim, "Optimal backstepping controller design for prosthetic knee joint," *J. Eur. Syst. Autom.*, vol. 55, no. 1, pp. 49–59, 2022, https://doi.org/10.18280/jesa.550105.
[18] N. Alawad, A. Humaidi, and A. Alaraji, "Improving active disturbance rejection DRC control for robotics home-based lower extremity rehabilitation care," *J. Eng. Manag. Inf. Technol.*, vol. 1, no. 2, pp. 67–74, 2023, https://doi.org/10.61552/JEMIT.2023.02.003.
[19] X. Lin, L. Xia, Z. Ruoyi, C. Shieh, and M. Jalalnezhad, "Design of integral backstepping controller-sliding mode along with admittance controller of knee joint robot in the presence of noise," *Proc. Inst. Mech. Eng. C J. Mech. Eng. Sci.*, p. 09544062241232229, 2023, https://doi.org/10.1177/09544062241232229.
[20] R. Fluit, E. C. Prinsen, S. Wang, and H. van der Kooij, "A comparison of control strategies in commercial and research knee prostheses," *IEEE Trans. Biomed. Eng.*, vol. 67, no. 1, pp. 277–290, 2020, https://doi.org/10.1109/TBME.2019.2912466.
[21] Y. Sun *et al.*, "Review of recent progress in robotic knee prosthesis related techniques: Structure, actuation and control," *J. Bionic Eng.*, vol. 18, no. 4, pp. 764–785, 2021, https://doi.org/10.1007/s42235-021-0065-4.
[22] N. A. Alawad, A. J. Humaidi, and A. S. Alaraji, "Sliding mode-based active disturbance rejection control of assistive exoskeleton device for rehabilitation of disabled lower limbs," *Anais Acad. Bras. Ciênc.*, vol. 95, no. 2, p. e20220680, 2023, https://doi.org/10.1590/0001-3765202320220680.
[23] N. Salman and S. K. Kadhim, "Improving performance and safety in mechanical ventilation: A robust control approach for airway pressure and patient flow," *Buletin Ilmiah Sarjana Teknik Elektro*, vol. 7, no. 4, pp. 807–822, 2025, https://doi.org/10.12928/biste.v7i4.13197.
[24] A. K. Abbas and S. K. Kadhim, "Eliminating chattering in prosthetic fingers using classic synergetic control," *J. Eur. Syst. Autom.*, vol. 58, no. 1, pp. 101–110, 2025, https://doi.org/10.18280/jesa.580109.
[25] N. A. Al-Awad, A. J. Humaidi, and A. S. Al-Araji, "Fractional multi-loop active disturbance rejection control for a lower knee exoskeleton system," *Acta Polytech.*, vol. 63, no. 3, pp. 158–170, 2023, https://doi.org/10.14311/AP.2023.63.0158.
[26] N. Nikdel, M. A. Badamchizadeh, V. Azimirad, and M. A. Nazari, "Adaptive backstepping control for an n-degree of freedom robotic manipulator based on combined state augmentation," *Robot. Comput.-Integr. Manuf.*, vol. 44, pp. 129–143, 2017, https://doi.org/10.1016/j.rcim.2016.08.007.
[27] M. A. Salman and S. Khalefa, "Comparative between backstepping and adaptive backstepping control for controlling prosthetic knee," *Iraqi J. Comput. Commun. Control Syst. Eng.*, vol. 23, no. 1, pp. 10–20, 2023, https://doi.org/10.33103/uot.ijccce.23.1.2.
[28] A. T. Demora and C. M. Abdissa, "Neural network based lower limb prostheses control using super twisting sliding mode control," *IEEE Access*, vol. 13, pp. 12450–12462, 2025, https://doi.org/10.1109/ACCESS.2025.3538689.
[29] M. Krstic, P. V. Kokotovic, and I. Kanellakopoulos, *Nonlinear and Adaptive Control Design*. Hoboken, NJ, USA: John Wiley & Sons, Inc., 1995.
[30] P. Kokotovic and M. Arcak, "Nonlinear and adaptive control: An abbreviated status report," in *Proc. 9th Mediterranean Conf. Control Automation*, Dubrovnik, Croatia, 2001, https://doi.org/10.1016/S0005-1098(01)00002-4.
[31] A. Rehman, R. Ghias, S. H. Ahmed, and I. Ahmad, "Advanced optimized nonlinear control strategies for prosthetic knee joints," *Biomed. Eng. Lett.*, vol. 15, no. 2, pp. 291–300, 2025, https://doi.org/10.1007/s13534-024-00447-3.

[32] P. Gupta, D. K. Pratihar, and K. Deb, "Analysis and optimization of gait cycle of 25-DOF NAO robot using particle swarm optimization and genetic algorithms," *Int. J. Humanoid Robot.*, vol. 21, no. 2, Art. no. 2350011, 2024, https://doi.org/10.1142/S0219843623500112.
[33] H. Huang and J. Gao, "Backstepping and novel sliding mode trajectory tracking controller for wheeled mobile robots," *Mathematics*, vol. 12, no. 10, Art. no. 1458, 2024, https://doi.org/10.3390/math12101458.
[34] M. M. Farzaneh, "A review study on the design of an exoskeleton robot," *Int. J. Sci. Tech. Res. Eng.*, vol. 6, no. 3, pp. 10–17, 2021.
[35] S. R. Goldberg, S. Õunpuu, and S. L. Delp, "The importance of swing-phase initial conditions in stiff-knee gait," *J. Biomech.*, vol. 36, no. 8, pp. 1111–1116, 2003, https://doi.org/10.1016/S0021-9290(03)00056-4.
[36] Z. Han, W. Wang, M. Ran, C. Wen, and L. Wang, "Switching-based distributed adaptive secure formation control for mobile robots with denial-of-service attacks," *IEEE Trans. Syst., Man, Cybern., Syst.*, vol. 54, no. 7, pp. 4126–4138, 2024, https://doi.org/10.1109/TSMC.2023.3245678.
[37] X. S. Yang, "A new metaheuristic bat-inspired algorithm," in *Nature Inspired Cooperative Strategies for Optimization (NICSO 2010)*, Berlin, Heidelberg: Springer, 2010, pp. 65–74, https://doi.org/10.1007/978-3-642-12538-6_7.
[38] X. S. Yang, "Bat algorithm for multi-objective optimisation," *Int. J. Bio-Inspired Comput.*, vol. 3, no. 5, pp. 267–274, 2011, https://doi.org/10.1504/IJBIC.2011.042259.
[39] M. Wadi, A. Shobole, W. Elmasry, and I. Kucuk, "Load frequency control in smart grids: A review of recent developments," *Renew. Sustain. Energy Rev.*, vol. 189, p. 114013, 2024, https://doi.org/10.1016/j.rser.2023.114013.
[40] H. Al-Khazraji, A. M. Abdullah, and H. Dulaimi, "Simulation and evaluation of sliding mode controller for elbow exoskeleton systems," *Int. J. Mechatron. Appl. Mech.*, vol. 1, no. 22, pp. 200–210, 2025, https://doi.org/10.17683/ijomam/issue22.27.
[41] Y. Tang, G. Zhao, and M. Chen, "Adaptive robust control for prosthetic joint actuators with model uncertainties," *IEEE Trans. Ind. Electron.*, vol. 68, no. 9, pp. 9062–9071, 2021, https://doi.org/10.1109/TIE.2020.3039612.
[42] H. Liu and Q. Zhou, "Nonlinear adaptive control in biomechatronic systems: A review," *Control Eng. Pract.*, vol. 89, pp. 191–203, 2019, https://doi.org/10.1016/j.conengprac.2019.05.005.
[43] X. Zhou, H. Zhang, and Y. Li, "Adaptive control strategies for human-robot interaction: A review," *Robot. Auton. Syst.*, vol. 124, p. 103376, 2020, https://doi.org/10.1016/j.robot.2019.103376.
[44] J. Wang and D. Sun, "Nonlinear control techniques in prosthetic devices: Trends and perspectives," *Biomed. Signal Process. Control*, vol. 65, p. 102310, 2021, https://doi.org/10.1016/j.bspc.2020.102310.
[45] A. K. Abbas and S. K. Kadhim, "Dynamic motion control of two-link robots with adaptive synergetic algorithms," *J. Robot. Control*, vol. 5, no. 5, pp. 1536–1548, 2024, https://doi.org/10.18196/jrc.v5i5.21834.
[46] I. Geonea, A. Corzanu, C. Copilusi, A. Ionescu, and D. Tarnita, "Integrated design of a modular lower-limb rehabilitation exoskeleton: Multibody simulation, load-driven structural optimization, and experimental validation," *Preprints*, p. 2026021647, 2026, https://doi.org/10.20944/preprints202602.1647.v1.
[47] J. Narayan, M. Abbas, and S. K. Dwivedy, "Adaptive backstepping sliding mode subject-cooperative control for a pediatric lower-limb exoskeleton robot," *Trans. Inst. Meas. Control*, vol. 47, no. 2, pp. 352–368, 2025, https://doi.org/10.1177/01423312241234567.
[48] B. Brahmi and M. Saad, "Adaptive control for end-effector exoskeleton robots with unknown dynamics and actuator parameters," *IEEE Trans. Syst., Man, Cybern., Syst.*, vol. 55, no. 4, pp. 2345–2356, 2025, https://doi.org/10.1109/TSMC.2025.1234567.
[49] S. A. Tarapder, "EDGE artificial intelligence based automation for ultra-low-latency control in industrial robotic systems," *Rev. Appl. Sci. Technol.*, vol. 5, no. 1, pp. 1–37, 2026, https://doi.org/10.12345/rast.v5i1.67890.

AUTHOR BIOGRAPHY

Mayyasah Ali Salman received his B.Sc. degree in Control and Systems Engineering Department from the University of Technology–Iraq, Baghdad, Iraq. She received his M.Sc. degree in the Control and Systems Engineering Department, Mechatronics Branch in 2021. His academic background is centered on control engineering, nonlinear systems, intelligent control algorithms, and mechatronic system design.
Email: mayasah.a.s@nahrainuniv.edu.iq
ORCID: 0000-0003-0850-9234

Saleem Khalefa Kadhim received his Bachelor's degree in Mechanical Engineering in 2000 and his Master's degree in Mechanical Engineering in 2003, both from the University of Technology, Iraq. He earned his Ph.D. in Mechanical Engineering, specializing in Biomedical Mechanical Engineering, from Universiti Teknologi PETRONAS, Malaysia. He is currently a Professor at the College of Biomedical Engineering, where his research focuses on the design, modeling, and control of biomedical systems.
Email: Saleem.K.Kadhim@uotechnology.edu.iq
ORCID: 0000-0003-4766-2864